

2D and 3D DOSY methods for studying mixtures of oligomeric dimethylsiloxanes

Marc J. Stchedroff,^a Alan M. Kenwright,^b Gareth A. Morris,^{*a} Mathias Nilsson^a and Robin K. Harris^{*b}

^a Department of Chemistry, University of Manchester, Oxford Rd, Manchester, UK M13 9PL.

E-mail: g.a.morris@man.ac.uk; Fax: (0)161 275 4598; Tel: (0)161 275 4665

^b Department of Chemistry, University of Durham, Durham, UK DH1 3LE.

E-mail: R.K.Harris@durham.ac.uk; Fax: (0)191 384 4737; Tel: (0)191 334 2021

Received 16th March 2004, Accepted 13th April 2004

First published as an Advance Article on the web 19th May 2004

Diffusion-ordered spectroscopy (DOSY) is a powerful method for the NMR analysis of many types of mixture without the need for physical separation, and requires only relatively standard spectrometer hardware. The principal requirements for high resolution analysis using DOSY, that the basic NMR spectrum be well-resolved and that it have good signal-to-noise ratio, pose a dilemma where multiple chemically similar species with NMR-active heteronuclei are involved. Generally the ¹H spectrum of such a mixture has good sensitivity but relatively poor chemical shift resolution, while for heteronuclei the situation is reversed. The dilemma is illustrated for the case of a mixture of cyclic dimethylsiloxanes, and the results of a range of ¹H 2D DOSY, ²⁹Si 2D DOSY and ¹H {²⁹Si} 3D DOSY–HMQC experiments are compared. In selecting the most appropriate technique to use for a given sample it is necessary to balance conflicting requirements for speed, resolution and accuracy, and to consider the balance between systematic and random errors. Results are presented for three different concentrations of a mixture of cyclic siloxanes containing between 4 and 20 monomer units. The diffusion coefficients measured show an inverse half power law relationship with molecular mass.

Introduction

Diffusion-ordered NMR spectroscopy (DOSY)^{1,2} uses pulsed field gradient spin or stimulated spin echo experiments to separate the NMR signals of the different components of a mixture on the basis of their diffusion characteristics. Experiments first dephase, and then, after a diffusion-encoding delay, rephase the nuclear magnetisation, using pulsed field gradients. A series of echo spectra are recorded with a range of gradient strengths, encoding information on diffusion coefficients into the attenuation of signals. Fitting the decay of signal amplitude to the expected Gaussian dependence on gradient strength allows a diffusion coefficient *D* and an associated error estimate σ_D to be obtained for each non-overlapping signal in a spectrum. A 2D DOSY spectrum can then be synthesised in which the 1D spectrum is extended into a second, diffusion, domain with signals dispersed with Gaussian lineshapes centred on the calculated diffusion coefficients *D* and with widths determined by the estimated errors σ_D . DOSY methods rely on obtaining clearly resolved NMR signals, so in crowded spectra it can be helpful to extend the experiment to a third dimension, a series of diffusion-attenuated 2D spectra being measured for different gradient strengths and a 3D DOSY spectrum then being synthesised. This paper examines the application of a range of different 2D and 3D DOSY techniques, several of them novel, to a mixture of cyclic dimethylsiloxane oligomers.

The chemistry of silicon, with its propensity for forming ring and cage structures through oxygen linkages, is a rich source of challenging problems in mixture analysis. The potential of ²⁹Si DOSY for unravelling the complex chemistry of alkaline aqueous silicate solutions has recently been illustrated;³ here some alternative strategies for investigating dimethylsiloxanes are explored. The relatively wide chemical shift range and long *T*₂'s of ²⁹Si in dimethylsiloxanes make directly-detected ²⁹Si

DOSY an attractive alternative to ¹H DOSY, the latter requiring extreme resolution enhancement if signals of similar dimethylsiloxane species are to be resolved. Unfortunately the relatively low receptivity of ²⁹Si limits the utility of directly-detected DOSY to concentrated samples; even with isotopic enrichment, sensitivity is far below that for ¹H. A useful palliative where suitable scalar couplings exist between ¹H and ²⁹Si is to use polarization transfer from protons to enhance the ²⁹Si signal.⁴ As well as giving the expected increase in available ²⁹Si spin-state polarization, this can give a significant further reduction in experiment duration because ¹H spin–lattice relaxation times are typically far shorter than those of ²⁹Si. It also allows diffusion encoding and decoding to be applied to ¹H rather than to ²⁹Si coherences, reducing the field gradients required by a factor γ_H/γ_S .

A further possibility is to exploit the two-bond couplings between ¹H and ²⁹Si in dimethylsiloxanes and use a DOSY–HMQC⁵ experiment, currently the highest resolution DOSY experiment available. The DOSY–HMQC experiment may be viewed either as a conventional ¹H 2D DOSY experiment to which ²⁹Si chemical shift encoding has been added, or as a ¹H–²⁹Si HMQC experiment incorporating diffusion weighting. The result is a 3D data matrix which, after double Fourier transformation, consists of a set of 2D HMQC spectra with different degrees of diffusion encoding. Measurement of corresponding cross-peak volumes in successive spectra then enables diffusion coefficients to be extracted by least squares fitting of the cross-peak decays.

Cyclic dimethylsiloxanes –((CH₃)₂SiO)_{*n*}– offer a useful test of DOSY methods; they show a smooth dependence of chemical shift on ring size,⁶ and with careful adjustment of field homogeneity it is possible to resolve signals from a wide range of species. The relative freedom of motion within the rings leads to both the ¹H and ²⁹Si spectra showing a single signal for each size of ring. In practice it is possible to resolve the

^{29}Si signals up to a ring size of about 16 units. For dilute solutions, the effective resolution in the ^1H spectrum is a little poorer, due to the reduced chemical shift dispersion; for concentrated solutions this degrades further because linewidths increase, chemical shift differences decrease, and experiments are complicated by the presence of radiation damping effects.⁷ ^1H DOSY is therefore best suited to dilute solutions of relatively small cyclic dimethylsiloxane oligomers, because of the limited chemical shift range and concentration-dependent resolution, while simple ^{29}Si DOSY without polarization transfer is restricted to very concentrated solutions or ^{29}Si enriched samples, because of the relatively low receptivity and long T_1 of ^{29}Si . Neither technique alone is directly applicable to the full range of concentrations. Using DEPT or INEPT polarization transfer to improve sensitivity and reduce recycle times extends the concentration range of ^{29}Si DOSY downwards by about an order of magnitude,⁴ but still requires relatively concentrated samples. DOSY–HMQC, on the other hand, has the potential to offer high resolution over a very wide range of concentrations, by exploiting both ^1H and ^{29}Si chemical shifts, but this can be at the expense of slightly less accurate diffusion measurements because of the difficulty of obtaining high purity 2D lineshapes. In this work three different samples were used, covering two orders of magnitude in concentration.

Pulse sequences

The basic pulse sequence used here for 2D DOSY was the oneshot sequence of ref. 8 (Fig 1a). However, the concentrations used for sample 2 were sufficiently high for radiation damping effects⁷ to be present (although not immediately apparent) in ^1H experiments. These effects took the form of a slight (tens of mHz) extra line broadening in normal ^1H DOSY experiments, and a significant distortion of the spectrum in which signals to higher and lower frequency of the midpoint of the band of dimethylsiloxane responses showed equal and opposite phase errors. Both effects increased with signal amplitude, and matched the known effects of radiation damping on multiplet signals.⁹ For sample 2, therefore, the modified oneshot sequence of Fig 1b was used¹⁰ for ^1H DOSY experiments; in this, the flip angle of the first pulse is reduced in order to decrease the net magnetization surviving the first part of the pulse sequence and hence avoid the damping and phase distortion of the resultant free induction decay.

Direct ^{29}Si observation requires very concentrated samples and long experiment times, particularly given the need to avoid any (negative) partial nuclear Overhauser effects. The sensitivity of ^{29}Si NMR can be markedly improved by polarization transfer,⁴ so an obvious expedient here is to use an experiment such as DOSY–DEPT or DOSY–INEPT.¹¹ In general INEPT¹² is preferable to DEPT¹³ for polarization transfer through small couplings such as those found in organosilicon NMR,⁴ because its lower overall duration leaves less scope for relaxation and homonuclear couplings to cause signal loss. The need to have relatively long precession periods within the polarization transfer sequence provides a very significant advantage in the context of DOSY, because it allows the diffusion encoding and decoding steps to be folded into the sequence. Previous polarization-transfer enhanced 2D DOSY experiments, and almost all existing 3D DOSY experiments, have used simple concatenation of existing pulse sequence building blocks to achieve their effect, for example prepending a pulsed field gradient stimulated echo to an HMQC sequence in DOSY–HMQC.⁵ In the experiments used here, diffusion encoding and decoding are added to both halves of the J -modulated ^1H echo component of the INEPT sequence. The use of two symmetrical diffusion-weighting segments in opposite sides of a spin echo sequence has an added advantage in cancelling some of the undesirable effects of main field

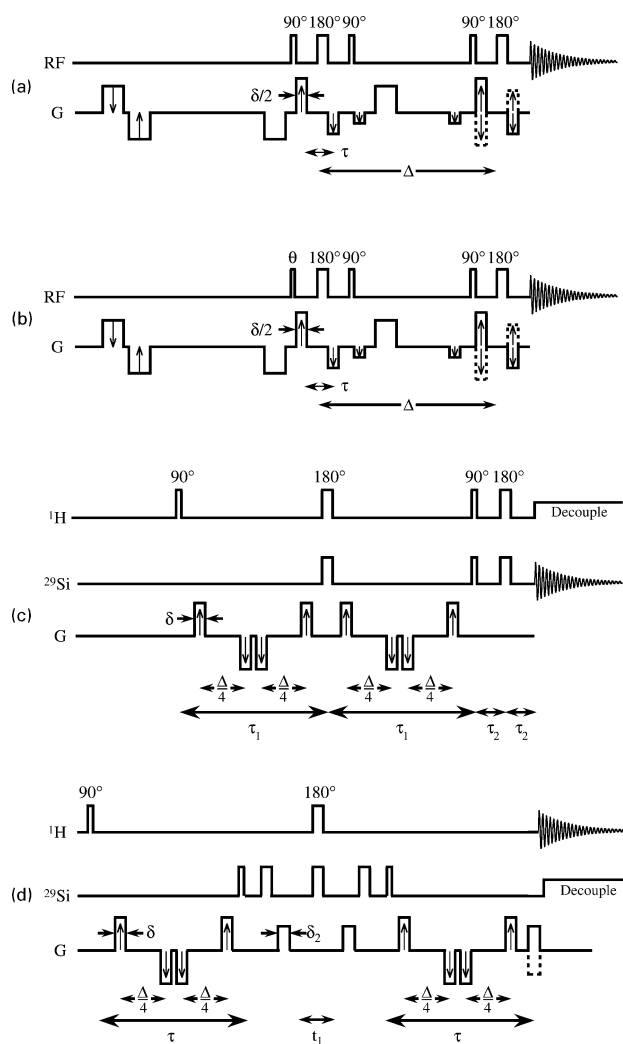


Fig. 1 Pulse sequences for 2D and 3D DOSY measurements. (a) “Oneshot” 2D DOSY sequence for direct observation;⁸ and (b) oneshot sequence modified to reduce radiation damping effects;¹⁰ (c) diffusion-weighted and convection-compensated INEPT sequence (INEPT–IDOSY); and (d) diffusion-weighted and convection-compensated phase sensitive gradient HMQC sequence (HMQC–IDOSY). In every case gradient pulses are followed by a recovery time of at least 1 ms. The phase cycling for sequences a and b is given in ref. 8; standard phase cycling was used for the INEPT and gHMQC pulse sequences c and d. Outward-facing vertical arrows in the gradient waveform G indicate a gradient strength that is incremented, and inward-facing decremented; in sequence d, F_1 quadrature detection is implemented by combining datasets acquired with the solid and dotted gradient waveforms.

disturbance by the gradient pulses. Because each delay uses a gradient echo, convection compensation^{14,15} can be added without any penalty in signal-to-noise ratio. The result is the INEPT–IDOSY pulse sequence of Fig. 1c, in which convection-compensated diffusion-encoded ^1H polarization is transferred to ^{29}Si . The suffix IDOSY here indicates that the diffusion weighting is internal to the INEPT sequence.

Existing DOSY–HMQC experiments are designed for correlating directly bonded carbon–proton pairs, and hence use only very short J -modulation delays. Here the leisure afforded by the relatively small (typically *ca.* 6 Hz) two-bond ^1H – ^{29}Si couplings once again allows diffusion weighting to be folded into the HMQC sequence, giving the HMQC–IDOSY sequence of Fig. 1d, in which convection-compensated gradient echoes are used to add two diffusion-encoding periods to HMQC. In both this case and that of the sequence of Fig. 1c, the direct incorporation of diffusion encoding into a heteronuclear coherence transfer sequence gives a substantial (more

than two-fold) sensitivity advantage over previous methods using stimulated echoes.

Experimental

Three samples containing different concentrations of mixtures of cyclic dimethylsiloxane oligomers, with the number of repeat units ranging from 4 up to about 20, were prepared. The synthesis of the cyclic species¹⁶ and their characterisation by ²⁹Si NMR⁶ have been described previously. The first sample (sample 1) consisted of a total of 0.7 ml containing approximately 75% dimethylsiloxane mixture and 25% deuteriobenzene by volume, and the second 45% v/v of a dimethylsiloxane mixture of slightly different composition and 55% deuteriobenzene. The third and most dilute solution (sample 3) consisted of a 1.1% w/w solution of sample 2 in deuteriobenzene, giving approximately 0.5% dimethylsiloxane mixture by volume. The approximate molar concentrations of individual cyclic species in the three samples were in the ranges 25–250 mM, 15–150 mM and 20–200 μM respectively.

Measurements were carried out on two Varian Unity INOVA narrow bore spectrometers, one at 500 MHz and the other 400, both equipped with Performa II gradient pulse amplifiers. Three different 5 mm probes were used, all with actively-shielded gradient coils. On the 500 MHz spectrometer a standard direct observation (normal geometry) broadband probe (probe 1) with a gradient coil delivering nominal gradients of up to 60 G cm⁻¹ was used. On the 400 MHz spectrometer one probe (probe 2) was a standard broadband indirect detection (inverse geometry) probe with a nominal 30 G cm⁻¹ gradient coil; the other (probe 3) was an extensively modified normal geometry broadband probe with a somewhat picaresque history. Originally a 400 MHz probe, it suffered a damaged capacitor and was in the process of being returned for repair when it was stolen. After being dumped in the Bridgewater canal it was recovered, washed, repaired, and modified for use at 300 MHz, where it provided a suitably challenging test for early work on gradient shimming.¹⁷ It was then converted back to 400 MHz and a 60 G cm⁻¹ gradient coil was added for the experiments described here. Probe 1 was used for direct observation ²⁹Si experiments on the most concentrated sample (sample 1), probe 2 for ¹H and 3D HMQC–DOSY experiments on sample 3, and probe 3 for all other experiments. Digital signal processing was applied to the data in real time. All experiments were carried out at room temperature (*ca* 21 °C), without temperature regulation but with the probe cooling air passed through a copper tube contained in a well-lagged water-filled bucket in order to ensure a constant probe temperature; previous observation has shown that this can maintain the probe temperature constant to better than ±0.1 °C over several hours.¹⁸ Automated *z*-gradient deuterium shimming¹⁷ was used prior to acquisition. Chemical shift referencing for experiments B to H followed the recent IUPAC guidelines.¹⁹

Proton-decoupled ²⁹Si 2D DOSY spectra of samples 1 and 2 were measured (experiments A and B) using the oneshot sequence of Fig. 1a with a diffusion-encoding gradient pulse imbalance factor α of 20%. No ¹H irradiation was applied during the recycle delay. For sample 1, 6 gradient increments were used in equal steps of nominal gradient squared from 2.6 to 37 G cm⁻¹ and 128 transients of 1024 complex points were acquired per gradient level in a total time of 13 h; the basic diffusion-encoding pulse duration δ was 4 ms and the diffusion time Δ 0.5 s. For sample 2, 10 gradient increments were used in equal steps of gradient squared from 2 to 50 G cm⁻¹ and 192 transients of 8192 complex points were acquired per gradient level in a total time of 54 h; the basic diffusion-encoding pulse duration δ was 3 ms and the diffusion time Δ 0.5 s. In both cases mild Lorentz–Gauss resolution enhancement was used; these and the subsequent oneshot 2D DOSY spectra

were synthesised by fitting peak height attenuation as a function of gradient strength $A(q^2)$ to the equation

$$A(q^2) = \exp[-q^2 D \{ \Delta + \delta(\alpha^2 - 2)/6 + \tau(\alpha^2 - 1)/2 \}] \quad (1)$$

and constructing a 2D spectrum in which each lineshape in the initial spectrum is extended into the diffusion dimension with a Gaussian lineshape centred on the fitted diffusion coefficient D and with a width determined by the standard error σ_D estimated in the fitting process.¹ If the pulsed magnetic field gradient may be treated as spatially uniform, the quantity q^2 is equal to $\gamma^2 g^2 \delta^2$, where γ is the magnetogyric ratio, g is the gradient strength, and δ is the basic diffusion-encoding gradient pulse duration. In practice, the magnitude of the gradient typically varies by 10–20% across the active volume of the sample, and for accurate diffusion measurements over a range of diffusion rates it is desirable either to replace g^2 in the expression for q^2 with a power series in g^{2n} , in which the coefficients are determined by mapping the field gradient distribution within the active volume of the probe,² or to replace eqn. (1) or its equivalent with a function tailored to the characteristics of the probe used.²⁰ In this work, the experiment carried out on sample 1 in probe 1 used the linear gradient assumption, with the gradient amplitudes calibrated according to the manufacturer's instructions (giving an estimated accuracy of 5% in gradient, 10% in D), while the remaining experiments used the power series method (typically improving accuracy approximately fivefold where the same pulse sequence is used for gradient mapping and for diffusion measurement).

A 2D ¹H decoupled ²⁹Si 2D DOSY spectrum of sample 2 was measured (experiment C) using the INEPT–DOSY sequence of Fig. 1c. 15 nominal field gradient amplitudes ranging from 2 to 60 G cm⁻¹ were used; for each, 32 transients of 2048 complex points were acquired, in a total experiment time of 1 h. The basic diffusion-encoding pulse duration δ was 2 ms and the total diffusion time Δ 40 ms. The proton echo time τ_1 was $0.25^3 J_{\text{SiH}} = 36$ ms, and the ²⁹Si echo time τ_2 was optimised at 8.2 ms. For the WALTZ proton decoupling during data acquisition, a very low radiofrequency field strength of 110 Hz was used in order to minimise sample heating and avoid convection. Data processing was as for the unenhanced ²⁹Si DOSY spectra, but fitting the results to the expression

$$A(q^2) = \exp[-q^2 D (\Delta - 4\delta/3)] \quad (2)$$

Proton 2D DOSY spectra of samples 2 and 3 were measured (experiments D and E) using the sequence of Fig. 1b for the concentrated sample 2 and that of Fig. 1a for the more dilute sample 3; in both cases data were fitted using eqn. (1) and WALTZ modulated ²⁹Si decoupling (again at a very low radiofrequency field strength of 200 Hz) was used to prevent the ²⁹Si satellites of one peak overlapping another and distorting the signal decay. For sample 2 an initial pulse flip angle of 15° was used; 8 transients of 1024 complex points were acquired for each of 15 gradient increments ranging from 2 to 32 G cm⁻¹, in a total experimental time of 26 min. For sample 3, 4 transients of 1024 complex points were acquired for each of 15 gradient increments ranging from 2.9 to 24.5 G cm⁻¹, in a total experimental time of 13 min. In both cases the basic diffusion-encoding pulse duration δ was 2 ms (*i.e.* each individual gradient pulse was of duration 1 ms) and the diffusion time Δ 150 ms.

3D HMQC–DOSY spectra of samples 2 and 3 were acquired (experiments F and H) using the pulse sequence of Fig. 1d with basic diffusion-encoding pulse durations δ of 2 ms and a total diffusion time Δ of 100 ms. For sample 2, 32 single transient t_1 increments each of 1024 complex points were acquired for 6 gradient strengths ranging from 2 to 32 G cm⁻¹, and processed with Lorentz–Gauss resolution enhancement in F_2 and Gaussian weighting in t_1 . The total data acquisition time for all 6 phase-sensitive 2D spectra was 42 min.

Sample 3 used similar parameters but with 4 transients and 128 increments, with 6 gradient strengths from 2.9 to 20 G cm⁻¹, and a total data acquisition time of 21 h. Diffusion coefficients were determined for each 2D peak by fitting the relative volumes of corresponding peaks in the 6 spectra with different field gradient pulse amplitudes to eqn. (2).

For comparison purposes, a ¹H 2D DOSY spectrum of sample 3 was measured (experiment G) using the pulse sequence of Fig. 1d to yield a ¹H DOSY spectrum filtered through the two-bond coupling between ¹H and ²⁹Si (the concomitant reduction in net ¹H magnetization observed obviates the need to reduce the flip angle of the initial pulse). The gradient pulse durations and diffusion time used were the same as those for the HMQC-DOSY experiment on this sample, while the gradient levels, number of transients, number of complex data points and total experimental time were the same as for the ²⁹Si-decoupled ¹H 2D DOSY spectrum.

Results

Table 1 lists the diffusion coefficients measured using the 8 experiments described above. The error limits quoted are twice the standard errors calculated by the Levenberg-Marquardt algorithm used for fitting the experimental data to eqn. (1) or (2), and offer an estimate of the errors in *relative* diffusion coefficients. The *absolute* accuracy of the diffusion coefficients measured is considerably poorer because of (a) uncertainties in gradient calibration (typically 10% for sample 1, better than half that for the remaining experiments), (b) uncertainties in temperature (typically giving rise to a 2–3% uncertainty in *D*), and (c) systematic errors caused by overlap between neighbouring peaks with different diffusion coefficients (small when signals are well-resolved, but can be 5% or more where peaks are extensively overlapped; see below). Of course, much larger systematic errors can result if care is not taken to prevent sample convection.

Fig. 2 shows the directly-observed ²⁹Si 2D DOSY spectrum obtained using the oneshot pulse sequence on the most concentrated sample (sample 1, experiment A) with a 500 MHz spectrometer (operating at 99.3 MHz for ²⁹Si). The 1D spectrum obtained for the lowest gradient strength is plotted at the top of Fig. 2 to show the normal ²⁹Si spectrum. Signals are

well-resolved for *n* = 4 to *n* = 14, but signals for *n* ≥ 15 are not resolved. Signals are reasonably narrow in the diffusion domain, the long time averaging and high magnetic field giving quite good signal-to-noise ratio and hence relatively low estimated errors in *D*. Experiment B gave qualitatively very similar results, the reduction in magnetic field strength and probe quality being compensated for by the more extensive time averaging, but with the lower concentration and hence reduced viscosity of sample 2 leading to an 80% increase in diffusion coefficient. The INEPT-IDOSY pulse sequence applied to the same sample (experiment C) gave the spectrum shown in Fig. 3, and yielded the same diffusion coefficients within experimental error, but with improved resolution in the diffusion domain and in one fiftieth of the time.

The ¹H spectrum of sample 2 is rather less well-resolved than the ²⁹Si, but offers much better sensitivity and hence can be used for more rapid measurements and more dilute samples. The ¹H 2D DOSY spectrum of Fig. 4 at first sight shows clear resolution of peaks until *n* = 13, with partially resolved peaks for *n* = 14 and *n* = 15, but on closer examination lacks any resolved peak for *n* = 4. As the HMQC spectrum shows (see Fig. 6 later), the ¹H chemical shifts for *n* = 4 and *n* = 5 in this sample are almost identical, and so these two peaks coincide. Turning to the most dilute sample, sample 3, the 2D ¹H DOSY spectrum of Fig. 5 shows significantly better resolution in both the spectral and diffusion dimensions, reflecting the wider range of chemical shifts and hence reduced signal overlap. The signal for *n* = 4 is now clearly separated from that for *n* = 5, and reasonable peak resolution is retained up to *n* = 15.

For samples intermediate in concentration between samples 2 and 3 (*ca.* mM), neither ²⁹Si 2D DOSY using the INEPT-IDOSY sequence nor ¹H using the oneshot sequence is entirely satisfactory: the former is too insensitive, the latter may fail to resolve the resonances of the two smallest rings. For all but the lowest concentrations, the experiment with the highest potential resolving power is HMQC-IDOSY, in which signals are resolved according to both ¹H and ²⁹Si chemical shifts before their attenuation is fitted to extract diffusion coefficients. Fig. 6 shows the first of the 6 HMQC spectra of experiment H, on sample 3, with the results of the diffusion fit marked for each peak. Such data may also usefully be plotted in 3D perspective form, as in Fig. 7. Here the projections of the 3D data

Table 1 Diffusion coefficients in units of 10⁻¹⁰ m² s⁻¹, with doubled standard errors σ_D calculated in the two-parameter exponential fitting of the signal attenuation data, for 8 different experiments A to H^a

Experiment	A ^b	B ^c	C ^c	D ^c	E ^c	F ^c	G ^c	H ^c
Sample	1	2	2	2	3	2	2	3
Nucleus observed	²⁹ Si	²⁹ Si	²⁹ Si	¹ H	¹ H	¹ H	¹ H	¹ H
Pulse sequence	Oneshot	Oneshot	INEPT-IDOSY	Oneshot	Oneshot	HMQC-IDOSY	1D HMQC-IDOSY	HMQC-IDOSY
<i>n</i>								
4	4.30 ± 0.22	7.74 ± 0.38	7.74 ± 0.08		11.51 ± 0.10	7.41 ± 0.12		11.64 ± 0.34
5	3.92 ± 0.09	6.99 ± 0.10	6.98 ± 0.06	(7.30) ± 0.06	10.46 ± 0.10	6.75 ± 0.02	(7.11 ± 0.06)	10.51 ± 0.26
6	3.65 ± 0.11	6.63 ± 0.05	6.51 ± 0.06	6.60 ± 0.08	9.71 ± 0.08	6.22 ± 0.03	6.51 ± 0.07	9.93 ± 0.21
7	3.30 ± 0.07	6.13 ± 0.08	6.17 ± 0.07	5.95 ± 0.12	9.03 ± 0.10	5.60 ± 0.03	6.05 ± 0.07	9.19 ± 0.25
8	3.11 ± 0.07	5.76 ± 0.26	5.84 ± 0.07	5.70 ± 0.06	8.40 ± 0.12	5.26 ± 0.04	5.58 ± 0.08	8.64 ± 0.19
9	2.95 ± 0.06	5.48 ± 0.33	5.48 ± 0.14	5.29 ± 0.11	8.07 ± 0.12	5.13 ± 0.05	5.25 ± 0.09	8.07 ± 0.17
10	2.80 ± 0.12	5.19 ± 0.27	5.25 ± 0.10	5.10 ± 0.08	7.65 ± 0.09	4.85 ± 0.05	4.95 ± 0.09	7.68 ± 0.14
11	2.72 ± 0.08	4.97 ± 0.30	5.02 ± 0.13	4.89 ± 0.07	7.35 ± 0.11	4.50 ± 0.03	4.80 ± 0.09	7.39 ± 0.10
12	2.65 ± 0.10	4.81 ± 0.17	4.81 ± 0.12	4.56 ± 0.10	7.13 ± 0.10	4.23 ± 0.03	4.63 ± 0.07	6.99 ± 0.17
13	2.54 ± 0.05	4.64 ± 0.18	4.60 ± 0.10	(4.32 ± 0.09)	6.80 ± 0.10	4.03 ± 0.02	4.32 ± 0.09	6.69 ± 0.26
14	2.45 ± 0.07	4.37 ± 0.14	4.40 ± 0.09	(4.06 ± 0.06)	6.46 ± 0.11	(3.99 ± 0.03)	(4.21 ± 0.06)	6.35 ± 0.22
15	(2.18 ± 0.07)	(4.36 ± 0.17)	(4.11 ± 0.07)	(3.78 ± 0.02)	6.11 ± 0.09	(3.72 ± 0.02)	(3.86 ± 0.09)	6.12 ± 0.08
16		(4.07 ± 0.13)	(3.91 ± 0.08)	(3.68 ± 0.04)	(5.67 ± 0.09)	(3.48 ± 0.03)	(3.48 ± 0.06)	(5.43 ± 0.49)
17					(5.32 ± 0.09)			(5.72 ± 0.11)
18					(4.80 ± 0.19)			(5.50 ± 0.68)

^a Bracketed figures are for signals showing severe overlap, where fitting the sum of two different decays leads to a compromise apparent diffusion coefficient. A, ²⁹Si oneshot, sample 1; B, ²⁹Si oneshot, sample 2; C, ²⁹Si INEPT-IDOSY, sample 2; D, ¹H oneshot, sample 2; E, ¹H oneshot, sample 3; F, HMQC-DOSY, sample 2; G, 1D HMQC-IDOSY (²⁹Si-filtered ¹H 2D DOSY), sample 2; H, HMQC-IDOSY, sample 3. ^b Experiment A was conducted on a 500 MHz spectrometer. ^c Experiments B to H on a 400 MHz instrument.

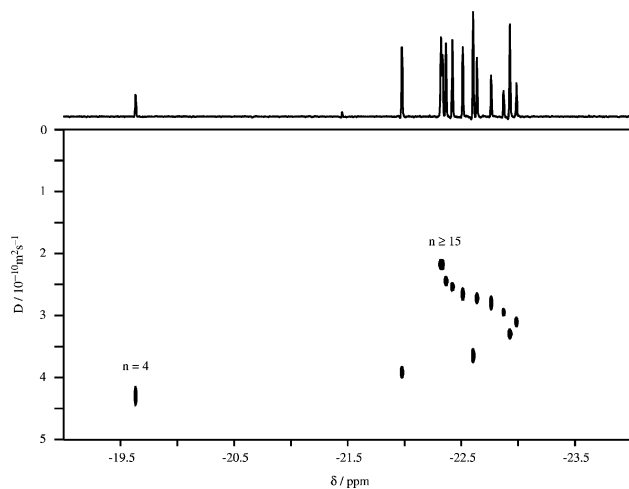


Fig. 2 ^{29}Si DOSY spectrum for the most concentrated sample (sample 1) of cyclic dimethylsiloxane oligomers measured in 13 h on a 500 MHz spectrometer with the oneshot pulse sequence of Fig. 1a, with (top) the normal ^{29}Si spectrum.

onto the ^{29}Si chemical shift/diffusion plane, the ^{29}Si chemical shift/ ^1H chemical shift plane and the ^1H chemical shift/diffusion plane are shown. The first of these is equivalent to the spectra of Figs. 2 and 3 (for samples 1 and 2 respectively), but was measured on sample 3, which is far too dilute for ^{29}Si signals to be measured directly.

The principal importance of DOSY is as an analysis tool for separating the NMR signals of different-sized species, but of course the diffusion coefficient values can also carry valuable information. As mentioned earlier, with careful calibration it is possible to obtain excellent diffusion accuracy using NMR methods. However, where multiple species are present, problems with signal overlap arise. These are particularly acute where, as in some instances here, the NMR signals are barely resolved. This places a premium on accurate adjustment of field homogeneity (shimming) and optimisation of data processing parameters such as resolution enhancement and baseline correction. The experiments carried out here may be divided into three classes. In experiments A and B (Figs. 2 and 3 respectively), signals are resolved according to ^{29}Si chemical shift. Signal-to-noise ratio is at a premium, but there is little or no overlap between signals up to $n = 14$ and so for most of the data the contribution of overlap to systematic errors is small. In experiments C, D and G (Figs. 4 and 5) proton spectra are measured, and the very small chemical shift differences

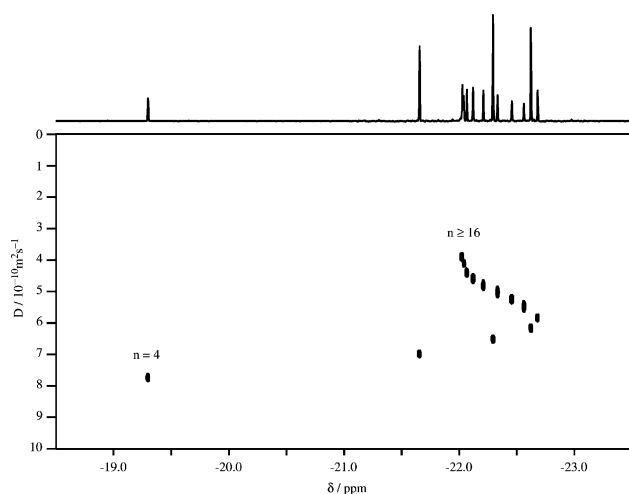


Fig. 3 ^{29}Si DOSY spectrum for sample 2, measured in 1 h on a 400 MHz spectrometer with the INEPT–DOSY pulse sequence of Fig. 1c.

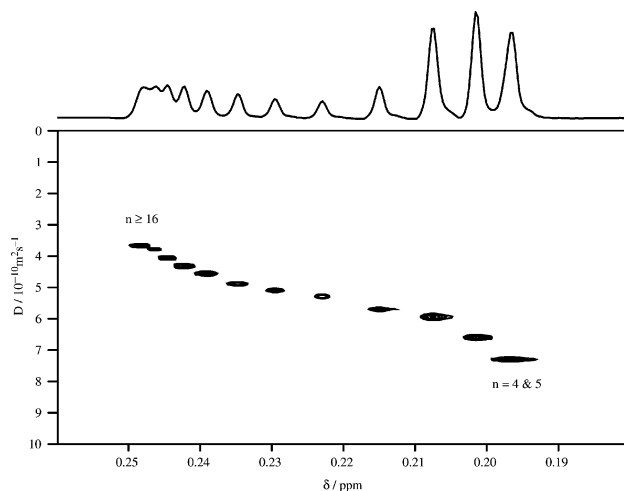


Fig. 4 ^1H DOSY spectrum for sample 2, measured in 26 min with the reduced initial flip angle oneshot pulse sequence of Fig. 1b.

make it impossible to avoid some overlap between the skirts of adjacent lines. The effect on the data can be insidious: chemical shift and diffusion coefficient both depend monotonically on ring size, so the changes in apparent diffusion coefficient caused by signal overlap do not lead to visible deviations from a smooth dependence of D on n .

In contrast, in the 3D HMQC–DOSY experiments F and H (Figs. 6 and 7) signal overlap leads to visible deviations of 5% or more from the expected behaviour. The ^{29}Si chemical shifts, unlike the ^1H shifts, do not vary monotonically with n , so that peaks from species of different sizes may show similar ^{29}Si shifts and hence the tails of these peaks overlap in one spectral dimension. At first sight this should not be a problem: signals are dispersed as a function of both ^{29}Si and ^1H chemical shifts and hence should be better resolved in the 3D DOSY experiments (based on 2D experimental spectra) than in the 2D (based on 1D experiments). This is indeed the case as far as the peaks proper are concerned, but the problem lies rather with the fringes of the 2D lineshapes. These show weak but broad ridges of positive and negative signal leading away from peaks along the two frequency axes, probably attributable largely to the transient perturbation of the static magnetic field by the field gradient pulses. In the great majority of multidimensional NMR experiments such effects are of little or no significance, since the data are relatively sparsely digitised in the two frequency domains. In the 3D HMQC–DOSY measurements made here, however, the need to obtain the best possible

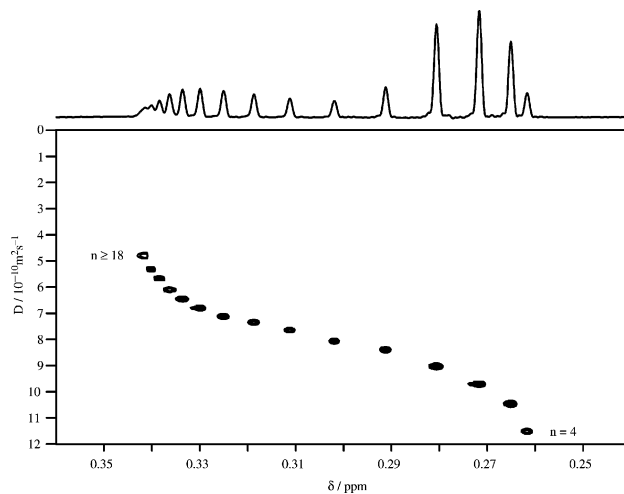


Fig. 5 ^1H DOSY spectrum for sample 3, measured in 13 min with the normal oneshot pulse sequence of Fig. 1a.

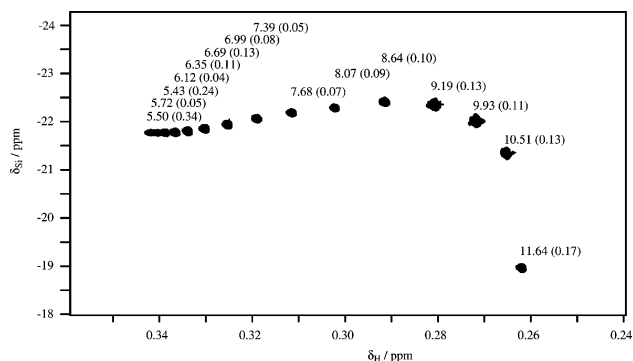


Fig. 6 HMQC spectrum for sample 3, measured using the HMQC–IDOSY sequence of Fig. 1d, annotated with the diffusion coefficients (and in brackets, the estimated standard errors) obtained by fitting the peak volumes in successive diffusion-weighted 2D spectra to eqn. (2).

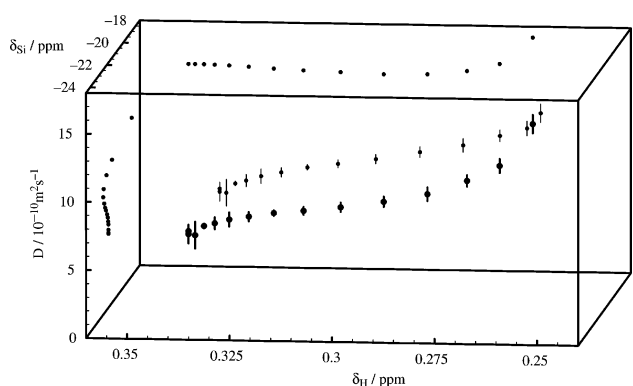


Fig. 7 3D representation of the results of experiment H (Fig. 6). Each cross-peak is represented by a solid sphere with a vertical line indicating the uncertainty in diffusion coefficient. The projections of the 3D data onto the 2D ^{29}Si chemical shift/diffusion plane, the ^{29}Si chemical shift/ ^1H chemical shift plane and the ^1H chemical shift/diffusion planes are also shown, corresponding to the ^{29}Si 2D DOSY spectrum (*cf.* Figs. 2, 3), HMQC spectrum (*cf.* Fig. 6) and ^1H 2D DOSY spectrum (*cf.* Figs. 4, 5) respectively.

spectral resolution leads to very well-digitised lineshapes and the effects of poor lineshape purity, exacerbated by the need for mild resolution enhancement, are clearly visible on spectra displayed with low contour thresholds. The effect of the overlap is to displace peak maxima slightly up or down depending on the particular combination of overlapping ridges, and hence to give the small erratic shifts in apparent diffusion coefficient visible on comparing diffusion coefficients in Table 1 measured by 2D and 3D methods on the same sample.

The diffusion coefficients of individual cyclic dimethylsiloxane oligomers have been investigated extensively in their own

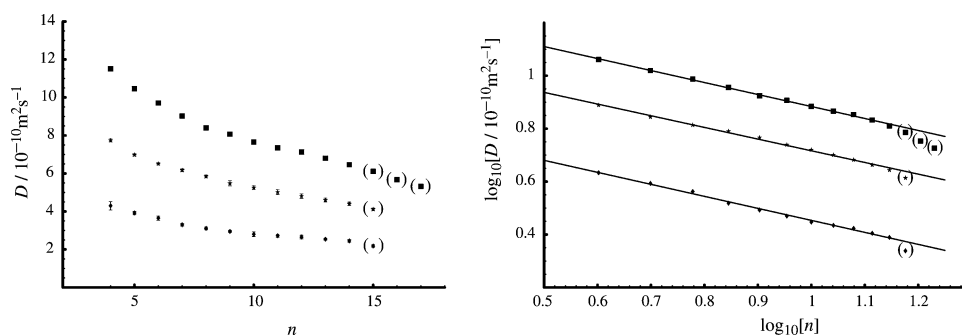


Fig. 8 Dependence of diffusion coefficient on ring size for the data of experiments A (sample 1, bottom), C (sample 2, middle) and F (sample 3, top); left, linear plot; right, decadic log–log plot. Apparent diffusion coefficients for signals which are significantly overlapped are shown in brackets, and were omitted from the linear least squares fitting of the data used to obtain the three straight lines shown.

right^{21,22} using the boundary-spreading technique. As the data of Fig. 8 show, the dependence of diffusion coefficient on ring size seen here for the three different benzene- d_6 solutions of dimethylsiloxane mixtures parallels that seen earlier in toluene and bromocyclohexane^{21,22} for samples containing only single species. All the data for non-overlapping signals fit well to a straight line in a log–log plot, showing that the diffusion coefficients scale approximately as the inverse square root of the ring size. This is the scaling expected both for a rigid highly oblate ellipsoid or thin disc²³ (an appropriate model for very small ring sizes) and for a cyclic random coil in a θ -solvent²¹ (appropriate for flexible rings). The straight lines in Fig. 8 are the result of fitting the non-overlapped experimental data for each of the samples 1 to 3, and show gradients of -0.45 ± 0.02 , -0.44 ± 0.02 and -0.45 ± 0.02 respectively. The experimental data thus show very similar behaviour over the full range from sample 1, where the individual species are effectively dissolved in their peers with only a small amount of benzene- d_6 present, to sample 3, in which the cyclic species are in dilute solution in benzene- d_6 . The gradients seen in the log–log plot differ slightly but significantly from the value of $-1/2$ expected for a random coil, but are well below the slope $-1/3$ seen where solvent is completely excluded from a folded chain (as for example in globular proteins), and are in good agreement with the gradient of -0.43 reported in ref. 21 for intermediate molecular weight cyclic poly(dimethylsiloxanes) in toluene.

Conclusions

All four types of experiment, ^1H DOSY, ^{29}Si DOSY, ^{29}Si INEPT–IDOSY, and ^1H $\{^{29}\text{Si}\}$ HMQC–IDOSY, show clear utility for the analysis of oligomeric systems such as these cyclic dimethylsiloxanes. The separation of signals according to diffusion coefficient allows easy assignment and size discrimination, with the effects of size differences of less than 10% readily seen in the diffusion dimension. The simple relationship between ring size and diffusion coefficient is potentially useful for the identification of rings of unknown size. The diffusion coefficients measured show that the behaviour of the individual components in this complex mixture of dimethylsiloxanes is very similar to that seen previously in monodisperse samples in other solvents. The power law relationship seen between diffusion coefficient and molecular mass is close to that expected for a cyclic random coil in a θ -solvent; the fact that the relationship is virtually unchanged on moving from a very concentrated to a very dilute solution suggests that differential solvation effects are not important in this system.

The choice between the different NMR techniques investigated here depends *inter alia* on the chemical shift ranges and relative receptivities of the nuclei involved, and the accuracy required. In the case of the cyclic dimethylsiloxane

oligomers studied here, HMQC–IDOSY gives good resolution and acceptable speed over a wide concentration range, ^{29}Si DOSY of concentrated solutions also gives good resolution but much more slowly, ^{29}Si INEPT–IDOSY is similar to ^{29}Si DOSY but about two orders of magnitude faster, and ^1H DOSY gives slightly poorer resolution very quickly for relatively dilute samples. The four techniques are affected to different extents by systematic errors originating in signal overlap, with HMQC–IDOSY the most vulnerable in systems where the highest spectral resolution is required. The HMQC–IDOSY results show that it is possible to obtain data with ^{29}Si chemical shift resolution for dilute solutions in a small fraction of the time needed for directly-observed experiments.

Acknowledgements

GAM thanks the EPSRC for grant GR/M16863. We thank Ian McKeag for his help in acquiring the 500 MHz data.

References

- 1 C. S. Johnson, Jr., *Prog. NMR Spectrosc.*, 1999, **3**, 203–256.
- 2 G. A. Morris, in *Encyclopedia of NMR*, ed. D. M. Grant and R. K. Harris, Wiley, New York, 2002, vol. 9, pp. 35–44.
- 3 R. K. Harris, K. A. Kinnear, G. A. Morris, M. J. Stchedroff, A. A. Samadi-Maybodi and N. Azizi, *Chem. Commun.*, 2001, 2422–2423.
- 4 J. Schraml, in *The Chemistry of Organic Silicon Compounds*, ed. Z. Rappoport and Y. Apeloig, Wiley, 2001, vol. 3, ch. 3.
- 5 H. Barjat, G. A. Morris and A. G. Swanson, *J. Magn. Reson.*, 1998, **131**, 131–138.
- 6 D. J. Burton, R. K. Harris, K. Dodgson, C. J. Pellow and J. A. Semlyen, *Polym. Commun.*, 1983, **24**, 278.
- 7 A. Abragam, *Principles of Nuclear Magnetism*, Oxford University Press, Oxford, 1961, pp 73–74.
- 8 M. D. Pelta, G. A. Morris, M. J. Stchedroff and S. J. Hammond, *Magn. Reson. Chem.*, 2002, **40**, S147–S152.
- 9 H. Barjat, G. P. Chadwick, G. A. Morris and A. G. Swanson, *J. Magn. Reson., Ser. A*, 1995, **117**, 109–112.
- 10 M. A. Connell, A. L. Davis, A. M. Kenwright and G. A. Morris, *Anal. Bioanal. Chem.*, 2004, **378**, 1568–1573.
- 11 D. Wu, A. Chen and C. S. Johnson, Jr., *J. Magn. Reson., Ser. A*, 1996, **123**, 215.
- 12 G. A. Morris and R. Freeman, *J. Am. Chem. Soc.*, 1979, **101**, 760–762.
- 13 D. M. Doddrell, D. T. Pegg and M. R. Bendall, *J. Magn. Reson.*, 1982, **48**, 323.
- 14 A. Jerschow and N. Müller, *J. Magn. Reson.*, 1997, **125**, 372.
- 15 N. Loening and J. Keeler, *J. Magn. Reson.*, 1999, **139**, 334.
- 16 K. Dodgson and J. A. Semlyen, *Polymer*, 1977, **18**, 1265.
- 17 H. Barjat, P. B. Chilvers, B. K. Fetler, T. J. Horne and G. A. Morris, *J. Magn. Reson.*, 1997, **125**, 197.
- 18 P. J. Bowyer, A. G. Swanson and G. A. Morris, *J. Magn. Reson.*, 2001, **152**, 234–246.
- 19 R. K. Harris, E. D. Becker, S. M. Cabral de Menezes, R. Goodfellow and P. Granger, *Pure Appl. Chem.*, 2001, **73**, 1795–1818.
- 20 P. Damberg, J. Jarvet and A. Gräslund, *J. Magn. Reson.*, 2001, **148**, 343–348.
- 21 C. J. C. Edwards, R. F. T. Stepto and J. A. Semlyen, *Polymer*, 1980, **21**, 781–786.
- 22 C. J. C. Edwards, R. F. T. Stepto and J. A. Semlyen, *Polymer*, 1982, **23**, 865–868.
- 23 C. Tanford, *Physical Chemistry of Macromolecules*, Wiley and Sons, NY, 1961, p. 327.